In terms of eq A-3 and A-5, eq A-7 and A-8 become

$$A = \frac{\sin \pi L_2 Y}{\pi Y} \tag{A-9}$$

and

$$B = e^{2\pi i(-(L_3/2)+x\cot\beta)Z} e^{\pi i L_3 Z} \frac{\sin \pi L_3 Z}{\pi Z} = e^{2\pi i x Z \cot\beta} \frac{\sin \pi L_3 Z}{\pi Z} \tag{A-10}$$

respectively. Finally, inserting (A-9) and (A-10) into (A-6) gives

$$F(XYZ) = \frac{\sin \pi L_2 Y}{\pi Y} \frac{\sin \pi L_3 Z}{\pi Z} \int_{-(L_1/2)\sin\beta}^{(L_1/2)\sin\beta} e^{2\pi i x(X+Z\cot\beta)}\, dx$$
$$= \frac{\sin [\pi L_1 \sin \beta(X + Z \cot \beta)]}{\pi(X + Z \cot \beta)} \frac{\sin \pi L_2 Y}{\pi Y} \frac{\sin \pi L_3 Z}{\pi Z} =$$
$$\frac{\sin [\pi L_1(X \sin \beta + Z \cos \beta)]}{\pi(X \sin \beta + Z \cos \beta)} \frac{\sin \pi L_2 Y}{\pi Y} \frac{\sin \pi L_3 Z}{\pi Z} \sin \beta \tag{A-11}$$

Further, by taking the approximation in terms of the Gaussian function[13]

$$\frac{\sin^2 (\pi X)}{(\pi X)^2} \doteq \exp(-\pi X^2) \tag{A-12}$$

the final expression for the amplitude $F(S)$, eq A-11, can be rewritten as (relative unit)

$$|F(S)|^2 = \exp\{-\pi[L_1^2(X \sin \beta + Z \cos \beta)^2 + L_2^2 Y^2 + L_3^2 Z^2]\} \sin^2 \beta \tag{A-13}$$

where $S = (X^2 + Y^2 + Z^2)^{1/2}$ is the scattering vector in reciprocal space.

## References and Notes


(1) Čačkovič, J. L.; Hosemann, R.; Čačkovič, H. *Kolloid Z. Z. Polym.* **1971**, *247*, 824.
(2) Hosemann, R.; Čačkovič, J. L.; Sassoui, M.; Weick, D. *Prog. Colloid Polym. Sci.* **1979**, *66*, 143.
(3) Čačkovič, J. L.; Hosemann, R.; Čačkovič, H.; Ferrero, A.; Ferracini, E. *Polymer* **1976**, *17*, 303.
(4) Ferrero, A.; Ferracini, E.; Čačkovič, J. L.; Čačkovič, H. *J. Polym. Sci., Polym. Phys. Ed.* **1984**, *22*, 485.
(5) Fronk, W.; Wilke, W. *Colloid Polym. Sci.* **1983**, *261*, 1010.
(6) Fronk, W.; Wilke, W. *J. Polym. Sci., Polym. Phys. Ed.* **1986**, *24*, 839.
(7) Ferracini, E.; Ferrero, A.; Čačkovič, J. L.; Hosemann, R.; Čačkovič, H. *J. Macromol. Sci.-Phys.* **1974**, *B10*, 97.
(8) Bonart, R.; Hosemann, R. *Kolloid Z. Z. Polym.* **1962**, *186*, 16.
(9) Hosemann, R.; Bagchi, S. N. *Direct Analysis of Diffraction by Matter*; North-Holland: Amsterdam, 1962.
(10) Kaji, K.; Mochizuki, T.; Akiyama, A.; Hosemann, R. *J. Mat. Sci.* **1978**, *13*, 972.
(11) Hosemann, R.; Čačkovič, J. L.; Kaji, K. *J. Appl. Crystallogr.* **1978**, *11*, 540.
(12) Wilke, W.; Göttlicher, K. *Colloid Polym. Sci.* **1981**, *259*, 596.
(13) Fronk, W.; Wilke, W. *Colloid Polym. Sci.* **1985**, *263*, 97.
(14) Hay, I. L.; Keller, A. *J. Mat. Sci.* **1967**, *2*, 538.
(15) Grubb, D. T.; Dlugosz, J.; Keller, A. *J. Mat. Sci.* **1975**, *10*, 1826.
(16) Keller, A.; Pope, D. P. *J. Mat. Sci.* **1971**, *6*, 453.
(17) Pope, D. P.; Keller, A. *J. Polym. Sci., Polym. Phys. Ed.* **1975**, *13*, 533.
(18) Gerasimov, V. I.; Tsvankin, D. Y. *Polym. Sci. USSR* **1969**, *11*, 3013.
(19) Gezalov, M. A.; Kuksenko, V. S.; Slutsker, A. I. *Polym. Sci. USSR.* **1970**, *12*, 2027.
(20) Crist, B. *J. Appl. Crystallogr.* **1979**, *12*, 27.
(21) Zheng, Z.; Nojima, S.; Yamane, T.; Ashida, T. *Polym. J.* **1989**, *21*, 65.
(22) Hall, I. H. *Structure of Crystalline Polymers*; Elsevier: England, 1984.
(23) Matyi, R. J.; Crist, B. *J. Polym. Sci., Polym. Phys. Ed.* **1978**, *16*, 1329.
(24) Vainshtein, B. K. *Diffraction of X-Rays by Chain Molecules*; Elsevier: Amsterdam, 1966.
(25) Wilke, W. *Acta Crystallogr.* **1983**, *A39*, 864.
(26) Dobb, M. G.; Johnson, D. J.; Majeed, A.; Saville, B. P. *Polymer* **1979**, *20*, 1284.
(27) Hindeleh, A. M.; Halim, N. A.; Ziq, K. A. *J. Macromol. Sci.-Phys.* **1984**, *B23*, 289.
(28) Zheng, Z. Thesis, 1989.
(29) Flory, P. J. *J. Am. Chem. Soc.* **1962**, *84*, 2857.


# One-Dimensional Aromatic Crystals in Solution. 10. A Helical Array of Anthryl Groups along a Polypeptide Chain


**Masahiko Sisido**†

*Research Laboratory of Resources Utilization, Tokyo Institute of Technology, 4259 Nagatsuta, Midori-ku, Yokohama 227, Japan.*

*Received February 9, 1989; Revised Manuscript Received March 30, 1989*


ABSTRACT: A sequential polypeptide having a repeating unit of [Lys(Z)-Lys(Z)-9-antAla] was synthesized [Lys(Z) = $^{\epsilon}N$-(benzyloxycarbonyl)-L-lysine; 9-antAla = L-9-anthrylalanine]. Circular dichroism of the polypeptide in solution showed a typical pattern of right-handed $\alpha$-helix at the amide absorption region. A very strong exciton splitting ($\Delta\epsilon_{248} = -217$; $\Delta\epsilon_{261} = +525$) was observed at the $^1$Bb absorption band of the anthryl group. The conformational energy calculation and the theoretical CD calculation indicated a one-dimensional array of the anthryl chromophores along the $\alpha$-helical main chain. The interchromophore center-to-center distance was predicted to be 7.2 Å. No strong ground-state interaction, such as dimer formation, was detected in the absorption and the fluorescence excitation spectra. Fluorescence spectra showed monomer and excimer fluorescence. It is suggested that very fast energy migration leads to efficient excimer formation.


Helical polypeptide chains have been used as the molecular framework along which a variety of chromophores can be arranged in a specific order and with specific spatial configurations.[1,2] Sequential polypeptides of the form I, containing L-1-naphthylalanine (napAla) [p($L_2$N)][3] or L-1-pyrenylalanine (pyrAla) [p($L_2$P)],[4] have been synthesized. The polypeptides were found to take $\alpha$-helical main-chain conformations[5] and the side-chain chromophores were shown to be arranged regularly along the helix.

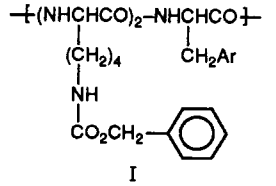


I

† Part of this work has been carried out at the Research Center for Medical Polymers and Biomaterials, Kyoto University.

0024-9297/89/2222-4367$01.50/0 

These polypeptides are the first examples of one-dimensional chromophoric arrays that exist in solution and probably in the solid state.

The present work is an extension of this line of study to synthesize a 9-anthryl derivative of I [p($L_2$A)]. The anthryl group possesses a very different electronic property from naphthyl and pyrenyl chromophores. Since the radiative transition between the lowest excited state ($^1$La) to the ground state is allowed for the anthryl group, a much stronger interchromophore interaction may be expected for the anthryl polypeptide than for the naphthyl or the pyrenyl one, whose lowest excited state is the forbidden $^1$Lb state.[6] The strong interchromophore interaction may lead to an efficient energy transfer or an electron transfer along the one-dimensional chromophoric array. For example, the Förster's critical distance for energy transfer ($r_0$) between 9-anthryl groups is 22 Å, whereas the $r_0$ value between pyrenyl groups is 10 Å.[7] If one assumes a one-dimensional array of chromophores with a spacing ($r$) of 7 Å, the single-step energy-transfer efficiency $\eta = r_0^6/(r^6 + r_0^6)$ is 0.999 for the anthryl group and 0.895 for the pyrenyl group. Then, the probability for the succeeding 50-step energy migration is 0.95 for the anthryl group, but it is 0.0038 for the pyrenyl group. This calculation predicts that the one-dimensional array of anthryl groups will be a very effective energy-transport medium.

Polymers carrying pendant anthryl groups have been reported.[8-10] In most of the polymers, however, the formation of ground-state dimers, excimers, and photodimers has been observed. For an effective energy transport, these structural defects, which may work as energy traps, must be excluded. In the anthryl polypeptide, the anthryl groups will be rigidly and regularly arranged along the helix with an appropriate interchromophore spacing, so these local defects will be suppressed to a minimum extent.

## Experimental Section

**Materials.** The sequential polypeptide I consists of '*N*-(benzyloxycarbonyl)-L-lysine and L-9-anthrylalanine (antAla). The synthesis and the optical purification of D-anthrylalanine has been reported previously.[11,12] The optical purification of the L isomer is first described in this paper.

The following abbreviations will be used: antAla = 9-anthrylalanine (L form, unless otherwise noted); Lys(Z) = '*N*-(benzyloxycarbonyl)-L-lysine; Z = benzyloxycarbonyl; Boc = *tert*-butyloxycarbonyl; Ac = acetyl; OMe = methyl ester; OSu = *N*-hydroxysuccinimide ester; EDC = 1-ethyl-3-[3-(dimethylamino)propyl]carbodiimide hydrochloride (water-soluble carbodiimide); HOBt = 1-hydroxybenzotriazole hydrate; TEA = triethylamine; MM = *N*-methylmorpholine; IBCF = isobutyl chloroformate; DMF = dimethylformamide; THF = tetrahydrofuran; TLC = thin-layer chromatography.

**Optical Purification of L-9-antAla.** Ac-DL-antAla and an equimolar amount of (−)-ephedrin were dissolved in hot ethanol. After a gradual cooling of the mixture, crystals precipitated. The crystals were found to be the diastereomeric complex of Ac-D-antAla and (−)-ephedrin. After the first crystals were filtered off, the second complex began to precipitate on cooling in a refrigerator. The two diastereomeric crystals could be discriminated by their crystal shapes. By repeating the above procedure, a pure diastereomer containing Ac-L-antAla was isolated. The free Ac-L-antAla was isolated from the optically pure diastereomer complex as described for the preparation of free D isomer. The optical purity was checked by the $^1$H NMR spectrum of antAla-OMe derivative measured in the presence of 0.4 mol equiv of a chiral shift reagent, tris[3-((trifluoromethyl)hydroxymethylene)-(+)-camphorato]Eu(III) in deuteriochloroform. No signal of the D isomer was detected in the NMR spectrum under the condition where racemic antAla-OMe exhibits two *O*-methyl signals. The circular dichroism (CD) of the free Ac-L-antAla-OH showed $[\theta]_{256} = -0.91 \times 10^5$ in ethanol. The deacetylation of the acetyl amino acid followed by the esterification was carried out as described before for the D isomer.[11]

**Boc-Lys(Z)-antAla-OMe.** Boc-Lys(Z)-OH (121 mg, 0.32 mmol) and antAla-OMe HCl (100 mg, 0.32 mmol) were dissolved in DMF (1.5 mL) and cooled with ice. EDC (0.067 mg, 0.35 mmol), TEA (0.049 mL, 0.35 mmol), and HOBt (0.064 mg, 0.48 mmol) were added to the mixture under cooling and the mixture was stirred at the ice temperature for 3 h and overnight at room temperature. An excess amount of ethyl acetate (30 mL) was added to the mixture and the solution was washed with water, 10% citric acid, 5% $NaHCO_3$, and water and dried on $Na_2SO_4$. The ethyl acetate was evaporated and the residue was solidified by the addition of ethyl ether: yield, 85 mg (42%); mp 87–92 °C. Anal. Calcd for $C_{37}H_{43}N_3O_7$: C, 69.25; H, 6.75; N, 6.55. Found: C, 69.52; H, 6.73; N, 6.38.

**Boc-Lys(Z)-antAla-OH.** Boc-Lys(Z)-antAla-OMe (70 mg, 0.11 mmol) was dissolved in methanol (1 mL) and 1 N NaOH (0.16 mL, 0.15 mmol) was added. The hydrolysis was followed by TLC (ethanol). It was almost completed after 7 h. The methanol was removed under vacuum. The residue was precipitated by the addition of aqueous NaCl solution. The precipitate was washed with ether to remove unreacted methyl ester and was dispersed in a 10% citric acid solution. The free acid was extracted with ethyl acetate and the extract was washed with NaCl solution repeatedly and dried on $Na_2SO_4$. Evaporation gave an oily product: yield 53 mg (78%).

**Boc-Lys(Z)-antAla-Lys(Z)-OSu.** Boc-Lys(Z)-OSu (Commercial) was dissolved in dioxane containing 3.5 N HCl. After 30 min, the dioxane was evaporated at room temperature. The residual oil was solidified by adding ethyl ether. The solid was repeatedly washed with ether and dried under vacuum. IR and NMR spectra were consistent with Lys(Z)-OSu HCl salt.

Boc-Lys(Z)-antAla-OH (53 mg, 0.085 mmol) and MM (9.3 μL, 0.085 mmol) were dissolved in THF (0.5 mL) and IBCF (11 μL, 0.085 mmol) was added at −15 °C. The mixture was stirred for 5 min at −15 °C and Lys(Z)-OSu HCl (35 mg, 0.085 mmol) and MM (9.3 μL, 0.085 mmol) dissolved in 0.2 mL of DMF were added. The mixture was stirred for 30 min at −10 °C and further for 2 h at room temperature. Excess amount of ethyl acetate was added to the mixture and the mixture was treated as in the case of Boc-Lys(Z)-antAla-OMe. The solid obtained was recrystallized from an ethyl acetate/ether mixture and washed with ether: yield 43 mg (51%); mp 150–151 °C. Anal. Calcd for $C_{54}H_{62}N_6O_{12}$: C, 65.71; H, 6.33; N, 8.51. Found: C, 65.98; H, 6.31; N, 8.43.

**Poly[Lys(Z)$_2$-antAla], p($L_2$A).** The Boc group of the oligopeptide *N*-hydroxysuccinimide ester was removed as in the case of Boc-Lys(Z)-OSu. The HCl salt obtained was washed with ethyl ether and dried under vacuum. The hydrochloride (21 mg, 0.022 mmol) was dissolved in freshly distilled DMF (0.1 mL) containing TEA (4.0 μL, 0.029 mmol) and the solution was stored in the dark for 1 week at room temperature. The polypeptide was precipitated by pouring the polymer solution into methanol and the precipitate was washed with a methanol/water mixture and methanol, yield 9 mg (50%). The polypeptide was subjected to a gel chromatographic analysis (Sephadex LH-60/DMF). All the fraction eluted at the elution limit of the gel, indicating the molecular weight is larger than about $10^4$.

**Measurements.** The spectroscopic measurements were made with freshly distilled trimethyl phosphate (TMP) as solvent. The solution was bubbled with argon gas for 10 min before each measurement. The following instruments were used: absorption, Hitachi 320; fluorescence, Hitachi F4000; CD, Jasco J-500; CPF, Jasco FCD-1.[13] The output of the spectrometers was interfaced to a personal computer (NEC PC9801), and the data were processed. A time-correlated, single-photon counting method was used to measure the fluorescence rise and decay curves. A synchronously pumped, cavity-dumped dye laser operated with a mode-locked Nd:YAG laser was an excitation source. The excitation wavelength was 350 nm.[14]

**Conformational Energy Calculation.** Programs for drawing energy contour maps, minimizing conformational energy by a Simplex procedure, and drawing molecular models, for peptides of any amino acid sequences including artificial amino acids, have been developed.[15] The programs were written on the MS-Fortran and run on an NEC PC9801 personal computer. The energy and structure parameters were taken from the ECEPP system.[16] The molecular models were drawn by using the NAMOD program

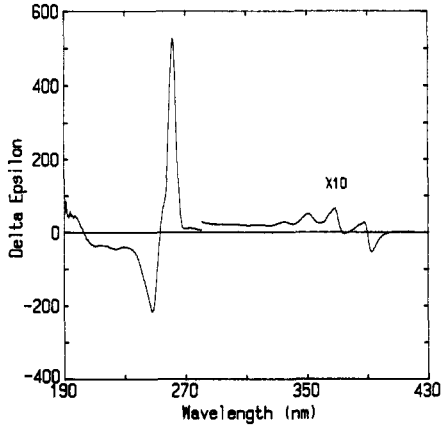


**Figure 1.** Circular dichroism of p($L_2$A) in TMP. [antAla] = 1.4 × $10^{-4}$ M; 1-mm cell; 25 °C.

(personal computer version) on an XY plotter.[17]

**Theoretical CD Calculation.** The theoretical CD was calculated on the basis of the exciton theory.[18] The computer program used to calculate the theoretical CD of p($L_m$N) was modified to include the anthryl chromophore.[3] The magnitude and the direction of the transition moments of an anthryl group were first taken from the results of PPP-CI MO calculation for anthracene.[19] The magnitudes of the transition moments were then modified to reproduce the experimental absorption spectrum of 9-ethylanthracene in TMP. The peak positions and the oscillator strengths employed in the present calculation were not much different from those previously determined with 9-anthrylmethyl acetate as the reference compound for the absorption spectrum.[19]

Each vibronic peak in the $^1$La or in the $^1$Bb band was considered as an independent transition having the same direction of the polarization. This assumption may be valid for the fully allowed $^1$Bb band but may not be a good approximation for the $^1$La band, which has a partially allowed character. Transition moments between the excited states ($^1$Lb–$^1$La, $^1$Bb–$^1$Lb) are also needed for the CD calculation. For these quantities, the PPP–CI results were used without modification. Besides the anthryl transitions, the amide $\pi\pi^*$ and $n\pi^*$ transitions were taken into account. These transition moments were taken from the literature.[20] For each rotational strength, a Gaussian function with a width of 5 nm (full width at half-maximum) was assigned and the smoothed curve was compared with the experimental spectrum. The computation was performed on a Hitachi M280 computer.

## Results and Discussion

**Circular Dichroism.** The conformation of aromatic polypeptide in solution is most conveniently studied by circular dichroism (CD). Figure 1 shows CD spectrum of p($L_2$A) in TMP. The ordinate is represented by the differential molar absorption coefficient $\Delta\epsilon = \epsilon_L - \epsilon_R$ with respect to the molar concentration of the anthryl groups. The $\Delta\epsilon$ with respect to the molar concentration of amide group is one-third of the ordinate of Figure 1. The CD around the amide absorption band (190–230 nm) shows a typical pattern of the right-handed $\alpha$-helix. The $\Delta\epsilon_{222}$ value, which is a good measure for the helix content, was −15.7 with respect to the amide group. Taking the contribution of much stronger negative exciton peak at 248 nm into account, the $\Delta\epsilon_{222}$ value is consistent with the value (−10.6 to −12.1) reported for the perfect $\alpha$-helical main chain.[21]

An exceptionally strong exciton couplet ($\Delta\epsilon_{248} = -217$, $\Delta\epsilon_{261} = +525$) was observed at the $^1$Bb absorption band of the anthryl group. These $\Delta\epsilon$ values are among the largest observed in solutions of molecularly dispersed substances. The CD is comparable to that observed for a cage-type compound carrying two rigidly fixed anthryl moieties, (6*R*,15*R*)-(+)-6,15-dihydro-6,15-ethanonaphtho-

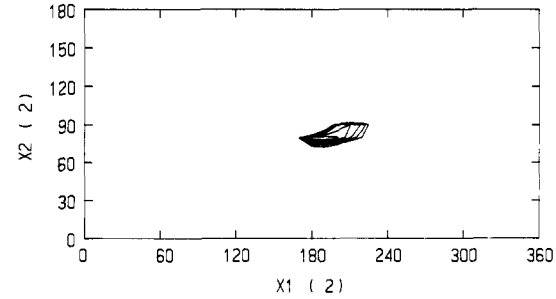


**Figure 2.** Energy contour map for the side-chain orientation of p($L_2$A), $n$ = 10. The interval of the contour lines is 1 kcal $mol^{-1}$.

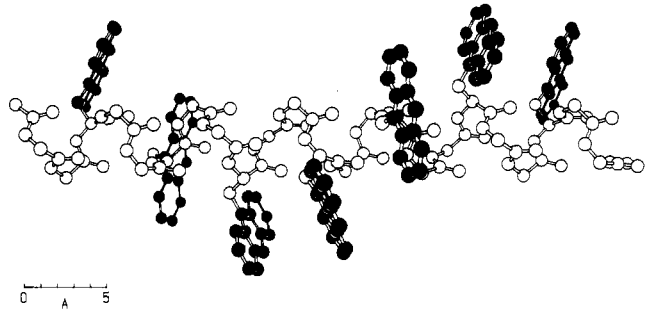


**Figure 3.** Most probable conformation of p($L_2$A). The main chain is an $\alpha$-helix ($\phi$ = −57°, $\psi$ = −47°, $\omega$ = 180°). The side-chain orientation is $\chi_1$ = 195°, $\chi_2$ = 75°. The interchromophore distance is 7.2 Å (center to center) and 4.7 Å (nearest edge to edge).

[2,3-*c*]pentaphene ($\Delta\epsilon_{249.7} = -360.4$, $\Delta\epsilon_{268} = 465.7$, with respect to one anthryl group).[22] The strong exciton couplet in the present polypeptide unequivocally indicates that the anthryl chromophores are arranged regularly and helically along the $\alpha$-helical main chain. A relatively small exciton splitting is also observed at the $^1$La band.

**Conformational Energy Calculation.** The CD data indicate that the main chain is a typical right-handed $\alpha$-helix and the side-chain anthryl groups are regularly arranged along the helix. The orientation of the anthryl group can be predicted from a conformational energy calculation for the [Ala-Ala-antAla] ($n$ = 10) polypeptide, where the Lys(Z) units have been replaced by alanine (Ala) units, for simplicity. The main chain was fixed to the right-handed $\alpha$-helix ($\phi$ = −57°, $\psi$ = −47°, $\omega$ = 180°), and a helical symmetry for the side-chain orientations were assumed during the calculation; i.e., all the side-chain rotational angles of the same type ($\chi_1$ or $\chi_2$) in the polypeptide were varied simultaneously. The $\chi_1$ (rotation of $C^\alpha$–$C^\beta$ bond) was varied from 0° to 360° at an interval of 10°. Taking the $C_2$ symmetry of the $C^\beta$–$C^\gamma$ bond into account, the $\chi_2$ was rotated from 0° to 180°. The side-chain energy contour map is shown in Figure 2.

Only a single orientation was found to be allowed for the anthrylmethyl group and the range of thermal fluctuation is very small ($\chi_1 = 190 \pm 8°$, $\chi_2 = 80 \pm 2°$) at room temperature (thermal energy < 1 kcal $mol^{-1}$). The contour map indicates that the anthryl side groups are forced to take a single orientation in the sequential polypeptide.

The most probable conformation of p($L_2$A) predicted from the calculation is illustrated in Figure 3. A one-dimensional array of anthryl chromophores along the polypeptide helix is seen. The center-to-center interchromophore distance between the nearest anthryl groups is 7.2 Å and the nearest edge-to-edge distance is 4.7 Å. The relative orientation of the anthryl group is favorable for the energy migration. The orientation factor $\kappa^2$ for the dipole–dipole energy transfer is

$$\kappa^2 = [\mathbf{e}_1\cdot\mathbf{e}_2 - 3(\mathbf{e}_1\cdot\mathbf{d})(\mathbf{e}_2\cdot\mathbf{d})]^2 \quad (1)$$

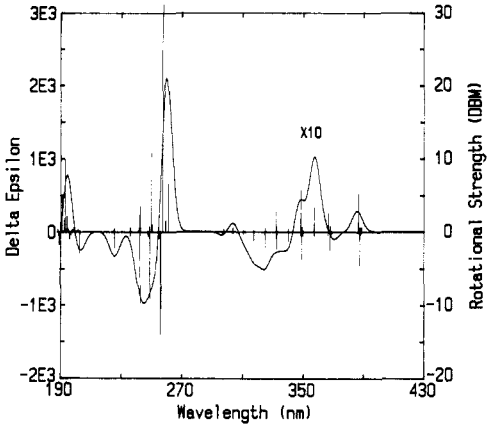


**Figure 4.** Theoretical CD spectrum of p($L_2$A) ($n$ = 10) in the most probable conformation shown in Figure 3. The sticks represent the rotational strength at each energy eigenvalue.

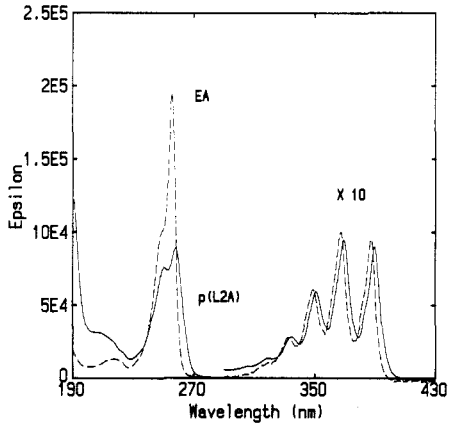


**Figure 5.** Absorption spectra of p($L_2$A) (—) and 9-ethylanthracene (- - -) in TMP. [antAla] = $1.4 \times 10^{-4}$ M; [EA] = $5 \times 10^{-5}$ M; 25 °C.

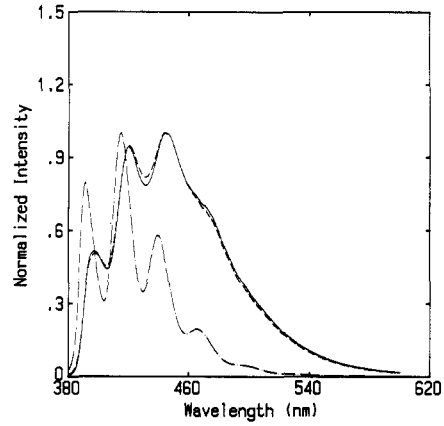


**Figure 6.** Fluorescence spectra of p($L_2$A) at 60 °C (—) and at 8 °C (- - -) in TMP, [antAla] = $5 \times 10^{-6}$ M. Fluorescence spectrum of 9-ethylanthracene (-·-) is also shown, [EA] = $5 \times 10^{-5}$ M at 25 °C. $\lambda_{ex}$ = 370 nm. The spectra are normalized at their maxima.

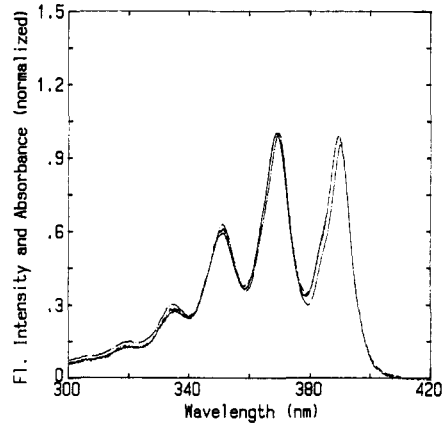


**Figure 7.** Fluorescence excitation spectra of p($L_2$A) monitored at 396 nm (—) and at 500 nm (- - -). The absorption spectrum of p($L_2$A) is (-·-) also shown. The three spectra are normalized at the peak around 370 nm. TMP solution.

where **d** is the unit vector connecting the centers of nearest anthryl groups and $\mathbf{e}_1$ and $\mathbf{e}_2$ are the unit vectors along the short axes of the two anthryl groups. The $\kappa^2$ was 1.27 for the side-chain orientation in Figure 3. This $\kappa^2$ value is about twice the value for random orientations ($^2/_3$).

**Theoretical Calculation of the Circular Dichroism.** On the basis of the geometrical structure of p($L_2$A) shown in Figure 3, a quantum-mechanical calculation of the CD spectrum was carried out for poly(Ala$_2$-antAla) ($n$ = 10). The result is shown in Figure 4. The sticks represent the rotational strengths at the corresponding energy eigenvalues. A Gaussian function of 5 nm (fwhm) was assigned to each stick and the theoretical CD curve was obtained as the sum of the all-Gaussian curves. The theoretical spectrum qualitatively reproduced the experimental one, especially at the $^1$Bb band. The shape of amide transition region (190–230 nm) may be fitted to the experimental curve, if a more broad Gaussian function was assigned to each rotational strength. The agreement was poor at the $^1$La absorption band (300–400 nm). The disagreement may be expected, since the polarizations of the $^1$La band may be different for each vibronic peak, due to the partially forbidden nature of the $^1$La band.

The intensity of the theoretical CD is higher than the experimental one by a factor of 4. Since the higher intensity of the theoretical CD than the experimental one has been calculated also for p($L_2$N),[3] it is not attributed solely to the fluctuation of the side-chain and the main-chain conformations. A likely reason for the overestimation may be the neglect of the higher order electronic interactions that are not taken into consideration. The higher order interaction is also apparent from the strong hypochromism observed in the absorption spectrum (Figure 5).[23]

From the results of experimental and theoretical CD spectra and the conformational calculation, p($L_2$A) takes on an $\alpha$-helical main chain and the anthryl chromophores are arranged in a one-dimensional array as shown in Figure 3.

**Absorption Spectrum.** The absorption spectrum of p($L_2$A) is compared with that of 9-ethylanthracene (EA) in Figure 5. Small red shifts are observed in p($L_2$A) at the $^1$La (2 nm) and the $^1$Bb (2.5 nm) band. In the $^1$Bb band, a marked hypochromism and a small splitting are observed. The magnitude of the Davydov splitting is 1230 cm$^{-1}$. These spectral data indicate that the anthryl chromophores interact in the one-dimensional array to form an exciton state in the $^1$Bb excited state.

Anthryl chromophores tend to form ground-state dimers when they are highly concentrated or densely attached to a polymer chain. The ground-state dimers have been found in polyesters[8,9] and poly($\beta$-arylmethyl L-aspartate)[10] carrying pendant anthryl groups, as an absorption around 410 nm. No such absorption is detected in p($L_2$A), indicating that the anthryl groups are rigidly fixed along the helix and the change of the interchromophore distance to form the dimer is prohibited. The absence of the ground-state dimer will be further confirmed by the fluorescence excitation spectrum (Figure 7).

**Fluorescence and Excitation Spectra.** The fluorescence spectra of p($L_2$A) and EA are shown in Figure 6. The spectrum of p($L_2$A) consists of the monomer fluorescence and the excimer fluorescence. The former is broadened and red-shifted from that of the model compound by 7 nm. The total (monomer + excimer) quantum yield at 25 °C is 0.48 for p($L_2$A) and 0.28 for EA ($\lambda_{ex}$ = 370 nm). A rough resolution of the polypeptide spectrum indicated that the quantum yield of the monomer fluorescence is about 0.13 and that of the excimer is about 0.35. The net increase of the total quantum yield is the consequence of the formation of the long-lived excimer and the absence of another quenching mechanism for the monomer excited state. The profile of fluorescence spectrum was independent of the excitation wavelength. This again indicates that no ground-state aggregates are present, which preferentially lead to the excimer.

Fluorescence excitation spectra were measured with two different monitor wavelengths (Figure 7). The two spectra coincided with each other and with the absorption spectrum. The coincidence again indicates the absence of the ground-state aggregates.

The temperature dependence of fluorescence spectrum of p($L_2$A) is shown in Figure 6. The total quantum yield decreased with increasing temperature (0.51 at 10 °C, 0.48 at 25 °C, and 0.41 at 60 °C). But no change in the spectral profile was observed over the range 10–60 °C. The temperature independence implies that the excimer/monomer ratio is not determined by any processes that require thermal activation, e.g., the deformation of the main chain and/or the side chain. The excimer/monomer ratio may be determined by other factors that are temperature insensitive. Among the possible candidates are a small amount of D isomers of antAla or Ala units incorporated in the polypeptide. The structural defect may enforce the neighboring anthryl pair to approach to form an excimer-forming site (EFS). The presence of only a little amount of the EFS may appear markedly in the fluorescence spectrum through an efficient energy transfer along the chromophoric array. Another possible EFS is the terminal portions of the chain, where the helix conformation is more or less unfolded.

The temperature independence of the excimer/monomer ratio of p($L_2$A) contrasts the case of p($L_2$P).[4] In the latter, the eximer/monomer intensity ratio increased monotonically with increasing the temperature from 10 to 60 °C by an approximate factor of 2. The different temperature dependence may be most reasonably interpreted in terms of the different mechanisms of the excimer formation. In the pyrenyl polypeptide the interchromophore center-to-center distance $r$ has been estimated to be 8.5 Å. Using the orientation-averaged Förster's critical distance for the energy transfer between pyrenyl groups ($r_0$ = 10 Å) and the intrinsic lifetime of the pyrenyl group in a polypeptide chain ($\tau_0$ = 200 ns),[24] a single-step energy-transfer rate constant $k = \tau_0^{-1}(r_0/r)^6$, is calculated to be $1.3 \times 10^7$ s$^{-1}$. The single-step energy-transfer rate constant for p($L_2$A) is calculated by using $r$ = 7.2 Å, $r_0$ = 22 Å, and $\tau_0$ = 8 ns. It is $1.0 \times 10^{11}$ s$^{-1}$ for random orientation and $2.0 \times 10^{11}$ s$^{-1}$ for the specific orientation shown in Figure 3. This rough estimation tells us that the excited state of pyrenyl group stays on the same chromophore for a long enough time (about 80 ns) to form an excimer with its neighboring pyrenyl groups by thermal fluctuations. On the other hand, the excited state of anthryl group does not stay on a specific chromophore for a long enough time to form an excimer. In the latter case, the excimer is formed after a multistep energy transfer or energy migration,

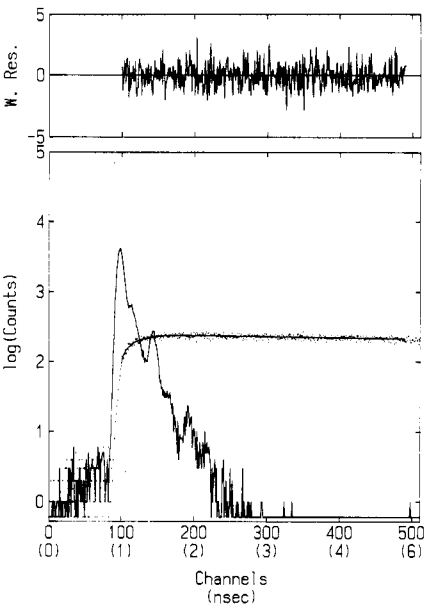


**Figure 8.** Fluorescence decay curve of p($L_2$A) monitored at the excimer fluorescence region ($\lambda_{ex}$ = 550 nm), in TMP at 20 °C. The best fit was obtained with a two-component exponential function: $I(t) = -0.31 \exp(-t/79\text{ ps}) + 0.43 \exp(-t/28\text{ ns})$; $\chi^2$ = 0.95.

followed by the trapping into an EFS. In this case, the excimer/monomer intensity ratio may become insensitive to temperature if the population of the EFS is temperature independent.

**Fluorescence Rise and Decay Curve Analysis.** The kinetics of excimer formation may be directly followed using time-resolved fluorometry. The excimer rise curve of p($L_2$A) is shown in Figure 8. The least-squares fitting indicated that the rise time is near the limit of the instrumental time resolution (about 80 ps). The short rise time of the excimer emission of p($L_2$A), together with the absence of ground-state dimers, supports the mechanism that a fast energy migration along the one-dimensional chromophoric array leads to efficient excimer formation.

Incidentally, a rise time of about 300 ps has been measured for the excimer emission of p($L_2$P). The longer rise time than that of p($L_2$A) supports qualitatively the picture described above. However, the rise time of p($L_2$P) is much shorter than the above rough calculation, indicating either that the thermal fluctuations of the pyrenyl groups are very brisk or that the energy migration among the pyrenyl groups is more frequent than expected, due to other mechanisms than the dipole–dipole one. This problem will be studied in the near future by using time-resolved fluorescence spectroscopy.

**Circularly Polarized Fluorescence Spectra.** The different mechanisms for the excimer formation of p($L_2$A) and in p($L_2$P) are further evidenced by the different structures of the excimers in the two polypeptides. The geometry of excimers formed in chiral systems can be studied in circularly polarized fluorescence (CPF) spectroscopy.[25] In p($L_2$P) the excimer exhibited a marked positive CPF signal ($g_{em} = 5 \times 10^{-3}$).[4] On the other hand, the excimer in p($L_2$A) showed no larger CPF signal than the limit of the instrumental accuracy ($g_{em} = 5 \times 10^{-4}$). The strong CPF signal in p($L_2$P) indicates that the excimer is formed in the helical part of the polypeptide by a small structural deformation. The absence of CPF signal in p($L_2$A) indicates that the excimer is formed at some locations where the helix structure is largely destroyed, e.g., the stereoirregular parts or the terminal portions. Therefore, the results of CPF spectra also support the

different mechanisms proposed for the anthryl and pyrenyl polypeptides.

## Conclusions

A sequential polypeptide carrying a one-dimensional array of anthryl chromophores was synthesized and characterized by experimental and theoretical CD spectroscopy. No ground-state dimer or higher aggregates was detected in the absorption and fluorescence excitation spectra. The fluorescence spectrum consisted of the monomer and the excimer fluorescence. It was shown that the excimer is formed after a very fast and efficient energy migration along the one-dimensional array. The EFS may be located where the helical structure is largely destroyed.

**Acknowledgment.** I thank Professor S. Tazuke and Dr. T. Ikeda for the use of the time-correlated single-photon counting apparatus. Financial support from the Ministry of Education, Science, and Culture, Japan (Grant-in-Aid for Scientific Research 63470095), is also acknowledged.

**Registry No.** p($L_2$A) homopolymer, 122334-92-3; p($L_2$A) SRU, 122357-51-1; Ac-DL-antAla, 82317-69-9; Ac-D-antAla·(−)-ephedrine, 106819-06-1; Ac-L-antAla, 109120-02-7; L-antAla-OMe, 122334-86-5; L-antAla-OMe·HCl, 122334-87-6; BOC-Lys(Z)-OH, 2389-45-9; BOC-Lys(Z)-antAla-OMe, 122334-88-7; BOC-Lys(Z)-antAla-OH, 122334-89-8; BOC-Lys(Z)-OSu, 34404-36-9; H-Lys(Z)-OSu·HCl, 64419-78-9; BOC-Lys(Z)-antAla-Lys(Z)-OSu, 122334-90-1; H-Lys(Z)-Lys(Z)-antAla-OSu·HCl, 122357-50-0; (−)-ephedrine, 299-42-3.

## References and Notes

(1) Sisido, M. *Makromol. Chem., Suppl.* **1985**, *14*, 131.
(2) Sisido, M. In *Photophysics of Polymers*; Hoyle, C. E., Torkelson, J. M., Eds.; ACS Symposium Series 358; American Chemical Society: Washington, DC, 1987; Chapter 26.
(3) Sisido, M.; Imanishi, Y. *Macromolecules* **1986**, *19*, 2187.
(4) Sisido, M. *Macromolecules*, in press.
(5) Yasui, S. C.; Keiderling, T. A.; Sisido, M. *Macromolecules* **1987**, *20*, 2403.
(6) Birks, J. B. *Photophysics of Aromatic Molecules*; Wiley-Interscience: London, 1970.
(7) Berlman, I. B. *Energy Transfer Parameters of Aromatic Compounds*; Academic Press: New York, 1973.
(8) Tazuke, S.; Banba, F. *J. Polym. Sci., Polym. Chem. Ed.* **1976**, *14*, 2463.
(9) Tazuke, S.; Hayashi, N. *J. Polym. Sci., Polym. Chem. Ed.* **1978**, *16*, 2729.
(10) Sisido, M.; Okamoto, A.; Egusa, S.; Imanishi, Y. *Polym. J.* **1985**, *17*, 1253.
(11) Egusa, S.; Sisido, M.; Imanishi, Y. *Bull. Chem. Soc. Jpn.* **1986**, *59*, 3175.
(12) Kawai, M.; Matsuura, T.; Butsugan, Y.; Egusa, S.; Sisido, M.; Imanishi, Y. *Bull. Chem. Soc. Jpn.* **1985**, *58*, 3047.
(13) Sisido, M.; Egusa, S.; Okamoto, A.; Imanishi, Y. *J. Am. Chem. Soc.* **1983**, *105*, 3351.
(14) Ikeda, T.; Lee, B.; Kurihara, S.; Tazuke, S.; Ito, S.; Yamamoto, M. *J. Am. Chem. Soc.* **1988**, *110*, 8299.
(15) Sisido, M., unpublished work.
(16) Momany, F. A.; McGuire, R. F.; Burgess, A. W.; Scheraga, H. A. *J. Phys. Chem.* **1975**, *79*, 2361.
(17) Beppu, Y. *Computers Chem.* **1989**, *13*, 101.
(18) Woody, R. W. *J. Polym. Sci., Macromol. Rev.* **1977**, *12*, 181.
(19) Sisido, M.; Okamoto, A.; Imanishi, Y. *Polym. J.* **1985**, *17*, 1263.
(20) Woody, R. W. *J. Chem. Phys.* **1968**, *49*, 4797.
(21) Walton, A. G. *Polypeptides and Protein Structure*; Elsevier: New York, 1981; Chapter 9.
(22) Harada, N.; Takuma, Y.; Uda, H. *J. Am. Chem. Soc.* **1976**, *98*, 5408.
(23) Rhodes, W. *J. Am. Chem. Soc.* **1961**, *83*, 3609.
(24) Sisido, M.; Tanaka, R.; Inai, Y.; Imanishi, Y. *J. Am. Chem. Soc.*, in press.
(25) Riehl, J. P.; Richardson, F. S. *Chem. Rev.* **1986**, *86*, 1.

# Determination of the Relaxation Spectrum by a Regularization Method

**J. Honerkamp* and J. Weese**

*Fakultät für Physik der Albert-Ludwigs-Universität, Hermann-Herder-Strasse 3, D-7800 Freiburg, FRG.* *Received January 25, 1989; Revised Manuscript Received April 14, 1989*

ABSTRACT: The determination of the relaxation spectrum using data from small amplitude oscillatory shear flow is investigated. Starting with the application of a linear regression method, the difficulties connected with the determination of the relaxation spectrum are illustrated. A new method based on classical Tikhonov regularization is proposed. The method has been tested using simulated experimental results. Finally it has been applied to the determination of the relaxation spectrum of a polybutadiene sample.

## 1. Relaxation Spectrum

The basic quantity in the linear theory for viscoelastic polymeric fluids is the relaxation module $G(t)$. It relates the stress tensor $\tau(t)$ to the rate of deformation tensor $\dot{\gamma}_{ij}(t) = \nabla_i v_j + \nabla_j v_i$ (where $v$ is the velocity field) in the constitutive

$$\tau(t) = \int_{-\infty}^{t} G(t - t')\, \dot{\gamma}(t')\, dt' \tag{1.1}$$

and it is directly measurable by a sudden shear displacement of the material ($\gamma(t) = \gamma_0\, \Theta(t)$, $\dot{\gamma}(t) = \gamma_0\, \delta(t)$). In the Rouse model[1] one obtains $G(t)$ as a sum of exponential terms

$$G(t) = \sum_{\alpha=1}^{M} e^{-t/\tau_\alpha} \tag{1.2}$$

where the $\tau_\alpha$ are specific relaxation times. A generalization of eq 1.2, which is also compatible with the expressions other models suggest for $G(t)$, is

$$G(t) = \sum_{\alpha=1}^{M} h_\alpha e^{-t/\tau_\alpha} \tag{1.3}$$

where the relaxation times $\{\tau_\alpha;\ \alpha = 1, ..., M\}$ are, for example, considered to be equally distributed on a logarithmic scale within an interval $[\tau_a, \tau_b]$. The $\{h_\alpha\}$ specifies the weight of each of these relaxation times.

The introduction of the relaxation spectrum $\{\tau_\alpha, h_\alpha\}$ corresponds with the discretization of the relaxation spectrum usually defined by the integral equation

$$G(t) = \int_{-\infty}^{+\infty} h(\tau)\, e^{-t/\tau}\, d \ln \tau \tag{1.4}$$

0024-9297/89/2222-4372$01.50/0 